



RELATION BETWEEN SPALL STRENGTH AND MESOPARTICLE VELOCITY DISPERSION

A. M. KRIVTSOV

St.-Petersburg State Technical University, Department of Theoretical Mechanics, Politechnicheskaya Street 29, 195251 St.-Petersburg, Russia. E-Mail: krivtsov@AK5744.spb.edu

Summary — From the plate impact experiments there were found out that the maximum spall strength corresponds just to the tests where the mesoparticle velocity dispersion is also maximum. In the paper computer investigation of this phenomenon is presented. Molecular dynamics method is used. It is shown that increase of the initial dispersion from zero to 15–25 m/s leads to the essentially increase of the material strength. The further increase of the initial dispersion leads to the slow decrease of the material strength, so the strength-dispersion characteristic has maximum.

INTRODUCTION

Impact loading of a plate target by a plate impactor from the same material is considered. The review articles [1, 2] provide access to most of the literature on this subject. The basic characteristics that can be measured in real time in spall fracture experiments are average velocity and dispersion of mesoparticle velocities on the free surface of the target [3, 4]. From real experiments it is known [4] that mesoparticle velocity dispersion appears to characterise an ability of the material to relax microstresses during the shock wave passage; and, thereby, it defines the macroscopic dynamic strength of material. The greater the mesoparticle velocity dispersion — the greater is the spall strength of the material. In the present paper, computer investigation of this phenomenon is presented. The simple molecular dynamics method is used [5, 6, 7]. The main distinction of the considered method from classic molecular dynamics is that the particles are interpreted not as atoms or molecules but as elements of the mesoscopic scale level. This approach shows a strong influence of mesoparticle velocity dispersion on the spall strength of material even for the simplest computation scheme.

METHODS

Since the purpose of this study is to understand the strength–dispersion relation generically, for molecular dynamics simulation a monoatomic two-dimensional lattice with standard Lennard-Jones 6–12 potential was chosen [6] as shown in (1)

$$U(r_{ij}) = \epsilon \left[\left(\frac{r_0}{r_{ij}} \right)^{12} - 2 \left(\frac{r_0}{r_{ij}} \right)^6 \right], \quad (1)$$

where $U(r_{ij})$ is the interaction energy between atoms i and j separated by distance r_{ij} , ϵ is the strength of the interaction, and r_0 is a characteristic length scale. In order to decrease calculation time, the potential is usually truncated at a finite distance, beyond which the interaction is taken to be zero. In the considered numeric experiments the cut-off distance was chosen to be $2.1 r_0$. In this case, the interaction potential has contributions from the first, second, and third nearest particles in the perfect crystal. However, the contribution of the second and the third neighbours to the total energy are minimal. Hence, r_0 is approximately the equilibrium, nearest-neighbour atomic separation. In order to describe nonelastic losses of energy small dissipative forces proportional to the particles velocities were added [8]. The simulation technique employed in this work is standard molecular dynamics method [5, 6, 9]: the trajectories of each atom are followed through time by integrating Newton's classical equations of motion. The integration is performed using the method of central differences [6]

The computational model is presented in Fig. 1. The particles are arranged in two rectangles lying in the xz plane. The rectangles represent the cross-sections of the impactor (black) and the target (grey). Initially the particles are arranged on a triangular lattice.

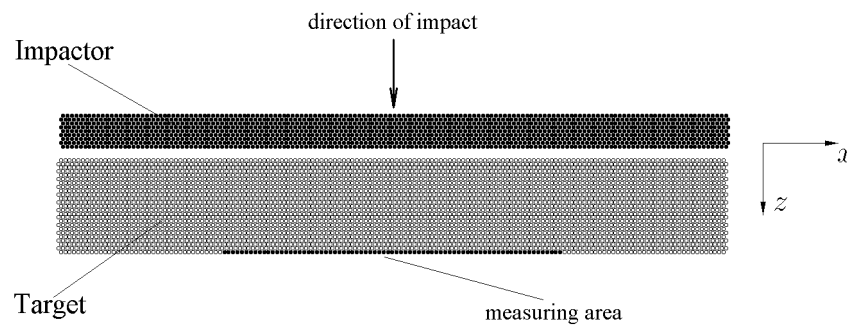


Fig. 1: The initial state of the pattern.

The lattice is orientated in such way that one of the sides of the triangles is extended along the x direction. The impactor is placed at an initial distance from the target greater than the cut-off distance of the interparticle potential. Both impactor and target are made from the same particles arranged on the same crystal lattice. The total number of particles in Fig. 1 is about 5000. Free boundary conditions on all boundaries were used.

Initially the target has zero velocity, the impactor has velocity directed along the z axis towards the target (see "direction of impact" in Fig. 1). In addition to the initial velocity of each particle a random velocity was added which was chosen from a two-dimensional random uniform distribution. Let us consider a set of particles indexed by $k = 1, 2, \dots, n$. Denoting V_k as projections of the particle velocities to the direction of impact, the mean velocity \bar{V} of the set in the impact direction is given by

$$\bar{V} = \frac{1}{n} \sum_{k=1}^n V_k. \quad (2)$$

The dispersion of the velocities is

$$\sigma = \frac{1}{n} \sum_{k=1}^n (V_k - \bar{V})^2. \quad (3)$$

Further the square root of the dispersion will be used

$$\Delta V = \sqrt{\sigma} = \sqrt{\frac{1}{n} \sum_{k=1}^n (V_k - \bar{V})^2}. \quad (4)$$

The quantity ΔV is the mean square deviation of the velocities (further — the deviation) and it has the dimensions of velocity. Given that at the initial moment of time, the impactor and target have the same initial dispersion, σ_0 , corresponding to the initial velocity distribution, then the initial deviation is $\Delta V_0 = \sqrt{\sigma_0}$. The aim of the presented computer experiments is to find out the dependence between the initial deviation and the strength characteristics of the material.

Let us note that if the particles are considered as elements of microscopic scale level — atoms or molecules, then the dispersion σ can be interpreted as the absolute temperature of the material. In our consideration, the particles correspond to elements of the mesoscopic scale level, The dispersion σ then corresponds to dispersion that is measured in real experiments [4] which differs from the classic temperature.

One of the main characteristics of the material strength is the spall strength [10] that is proportional to the spall (pull-back) velocity W . The spall velocity can be calculated from the time relation of the average velocity on the free surface [4, 10]. To find out the average velocity and other characteristics on the free surface we shall use the central part of the last particle row of the target (see Fig. 1, “measuring area”). The length of the area is one-half of the total row length to avoid boundary effects.

Another characteristic that will be used to describe the strength of the material is the width h of the spall crack in the impact direction — see Fig. 2. The technique of the crack

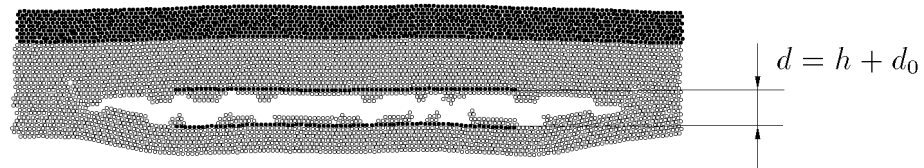


Fig. 2: Measuring of the width of the spall crack.

width measuring in the presented computer experiments as follows. Two rows — above and below the place where the crack appears — are selected in the initial state of the pattern. The averaged distance d_0 between the rows at $t = 0$ is measured. Then, during the experiment ($t > 0$) the time relation of the averaged distance $d(t)$ is measured (Fig. 2). Then time dependence on the crack width can be obtained as

$$h(t) = d(t) - d_0.$$

To avoid the boundary effects, only the central part of the rows (one-half of the total length) is used for measurement. In Fig. 2 the pattern with crack is shown — rows used for the measurement are coloured black. Note that the presented method can be used in the situation where there are a lot of small microcracks — in this case it gives the integral width of the microcracks.

RESULTS

To clarify our results, the same scales of time, distance and velocity in the computer calculations are used as in the real experiments with ductile steels [4]. We chose the following sizes: impactor thickness (z size) is 2 mm, target thickness is 7 mm, impactor width (x size) is 52 mm, target width is same with the impactor width. In Fig. 3–4 results of the computer experiments are presented. The pattern consists of about 5000 particles. All experiments

were performed with the same impactor velocity — 260 m/s. The initial velocity deviation ΔV_0 was varied from 0, 1, 2 to 100 m/s. Every row in Fig. 3–4 corresponds to some value of deviation. The first column shows the pattern state at $t = 4.1 \mu\text{s}$ ($t = 0$ corresponds to the first contact between impactor and target). Note that the greatest crack size is realised at $\Delta V_0 = 0$. While the deviation increases, the crack width becomes smaller and at $\Delta V_0 = 25 \text{ m/s}$ crack completely disappears. The dispersion increase has absolutely prevented the spall fracture! When deviation ΔV_0 is in range of 25 – 40 m/s there is no spall fracture. For $\Delta V_0 > 40 \text{ m/s}$ the crack appears again and increases while the deviation grows. At deviation value of 100 m/s we can see fracture of the pattern produced with the high level of dispersion (this effect is analogous to temperature fracture).

The second column in Fig. 3–4 shows time dependence of the free surface velocity. The third column in Fig. 3–4 shows time dependence of the crack width h . Note that the deviation increase leads to a lowering of the crack width, especially for the times $t > 3 \mu\text{s}$. For small deviations (0–2 m/s), the $h(t)$ dependence is monotonic. This means that the crack grows during all the time of measurement. For greater values of deviation the $h(t)$ dependence has one or two maximums after which the crack width decreases. Therefore we have the effect of recovering of the material — high level of dispersion stimulates relaxation processes.

Thus from the computer experiments it follows that a material with greater dispersion is stronger. Why is this so? To make it clear let us consider Fig. 5, where patterns are shown for two moments of time. The left column corresponds to $t = 1.4 \mu\text{s}$, it is shortly after the time when the fracture starts. The right column shows the pattern state after the crack formation ($t = 4.1 \mu\text{s}$). The rows, as it was before, correspond to the different values of the initial deviation ΔV_0 .

From the first row of Fig. 5, note that when the deviation is absent ($\Delta V_0 = 0$) the crack borders are absolutely straight. When the deviation increases then the crack borders become more and more irregular (the right column). Now look to the left column to see how the fracture appears. For $\Delta V_0 = 0$ there is only one long crack, but for $\Delta V_0 = 4 \text{ m/s}$ we have a lot of short microcracks. Thus, the dispersion leads to smearing of the shock wave, and it is the reason why the strength increases. Note that at $\Delta V_0 = 20\text{--}25 \text{ m/s}$ the microcracks that are present at $t = 1.4 \mu\text{s}$ disappear at $t = 4.1 \mu\text{s}$. The small cracks can disappear spontaneously — this is one more reason for the strength increase.

The same experiments for the more complicated model containing about 20000 particles are shown in Fig. 6. The impactor velocity is 297 m/s. The results are similar, but effect of the strength increase is sharper: already at $\Delta V_0 = 9 \text{ m/s}$ no crack appears. The great values of dispersion, as it was for 5000 particles, decrease the material strength — the spall crack appears at $\Delta V_0 = 30 \text{ m/s}$ and became larger while ΔV_0 increases up to 100 m/s.

Experiments with 20000 particles produce better time relations for the free surface velocity — see the second column in Fig. 6. The form of the curves is in good agreement with results of real experiments and theoretical calculations [4, 11]. In the first four graphs ($0 \leq \Delta V_0 \leq 4 \text{ m/s}$) after the first maximum of the velocity-time relation note the oscillations in the spall plate. Note that dispersion minimises the amplitude of the oscillations. After $\Delta V_0 = 9 \text{ m/s}$ there is no spall — and no oscillations in the spall plate. At these deviations a new maximum appears — the wave of compression that has reflected from the free surface of the impactor, crossed the whole width of the pattern, and appears at the free surface of the target. For the high values of dispersion ($\Delta V_0 \geq 40 \text{ m/s}$) we have the spall again, and again it is possible to see the oscillations in the spall plate, but with very low amplitude. At $\Delta V_0 > 60 \text{ m/s}$ dispersion almost suppresses the oscillations.

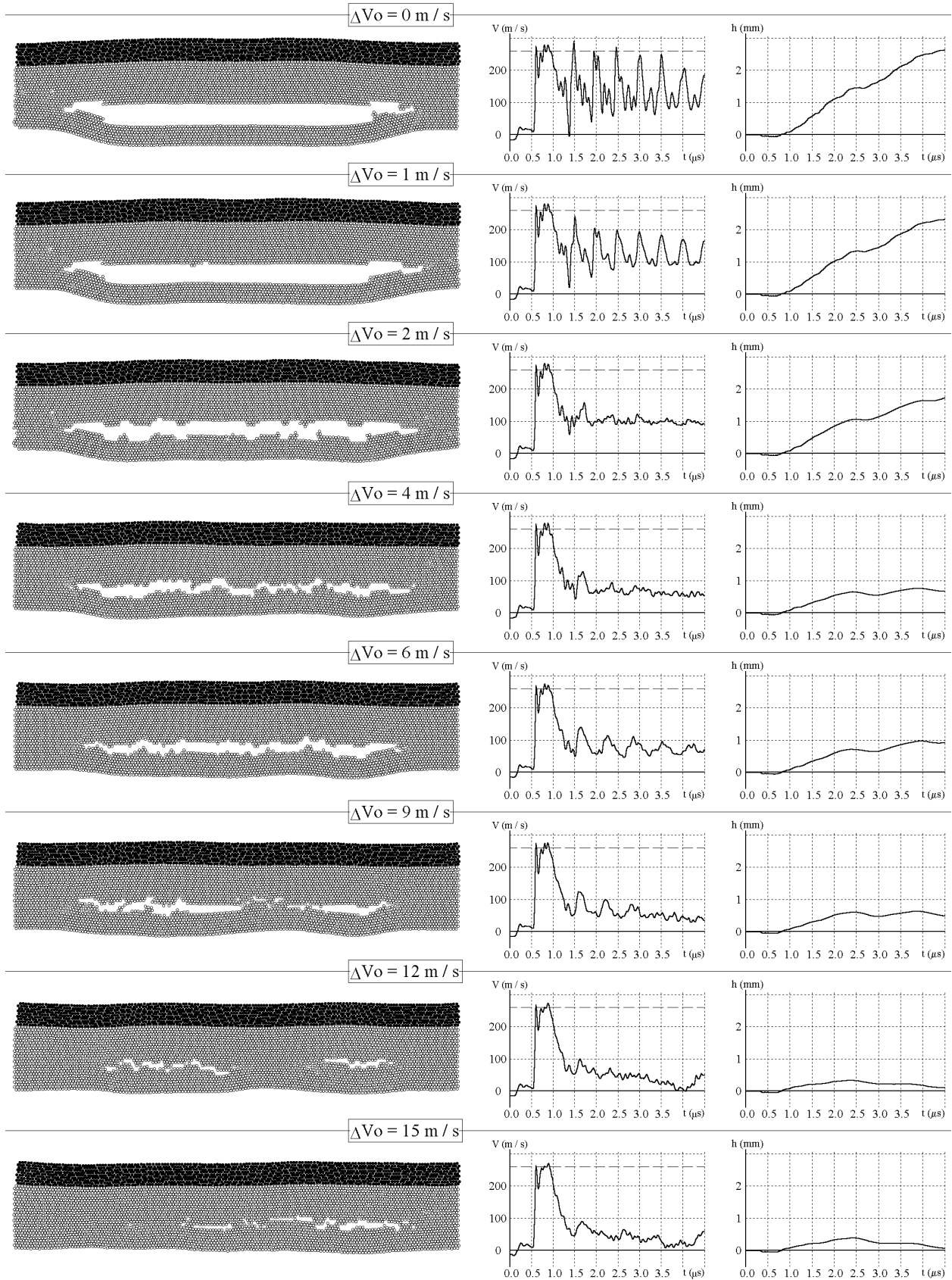


Fig. 3: Computer results for $0 \leq \Delta V_0 \leq 15$ m/s, 5000 particles.

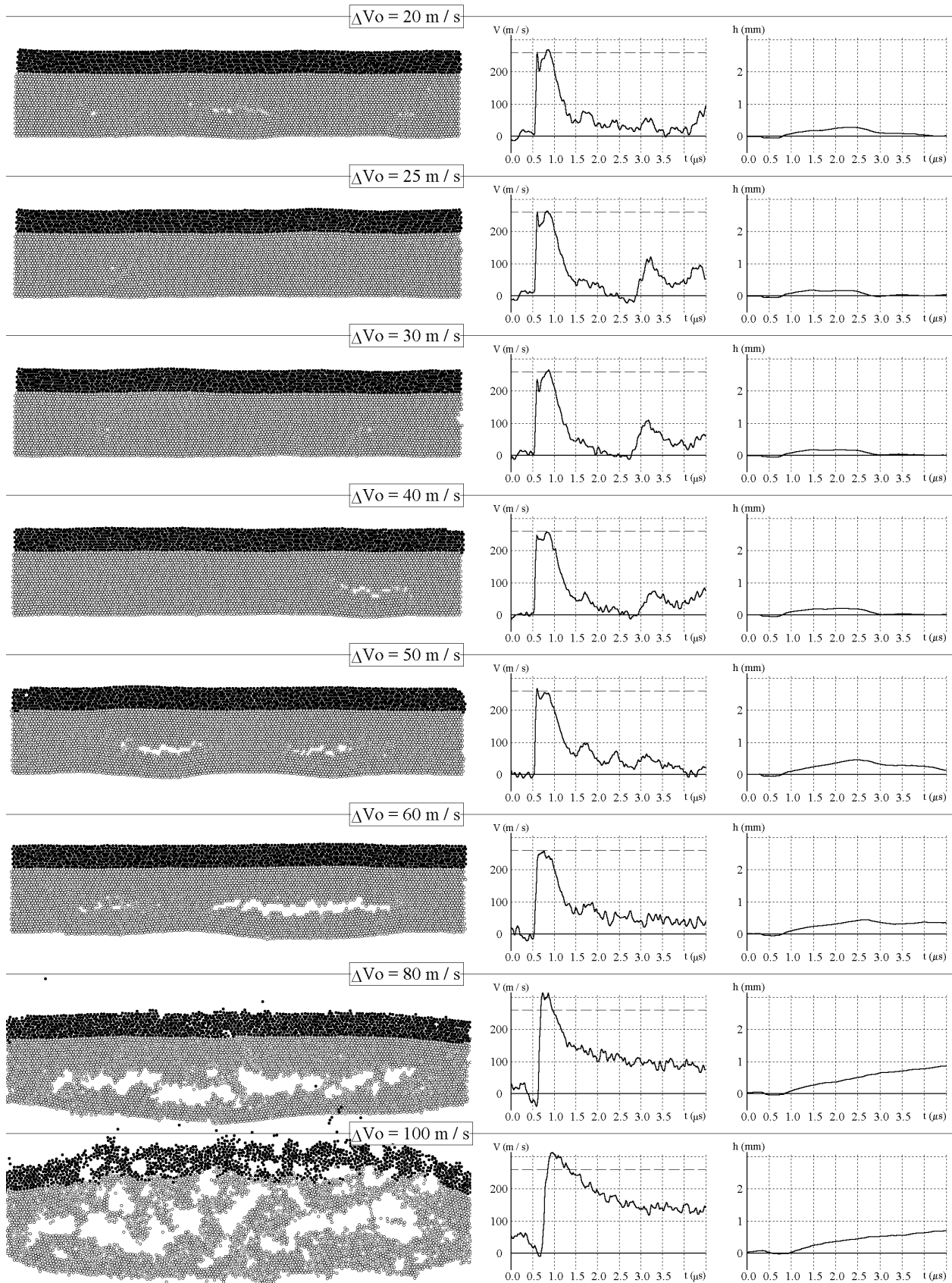


Fig. 4: Computer results for $20 \text{ m/s} \leq \Delta V_0 \leq 100 \text{ m/s}$, 5000 particles.

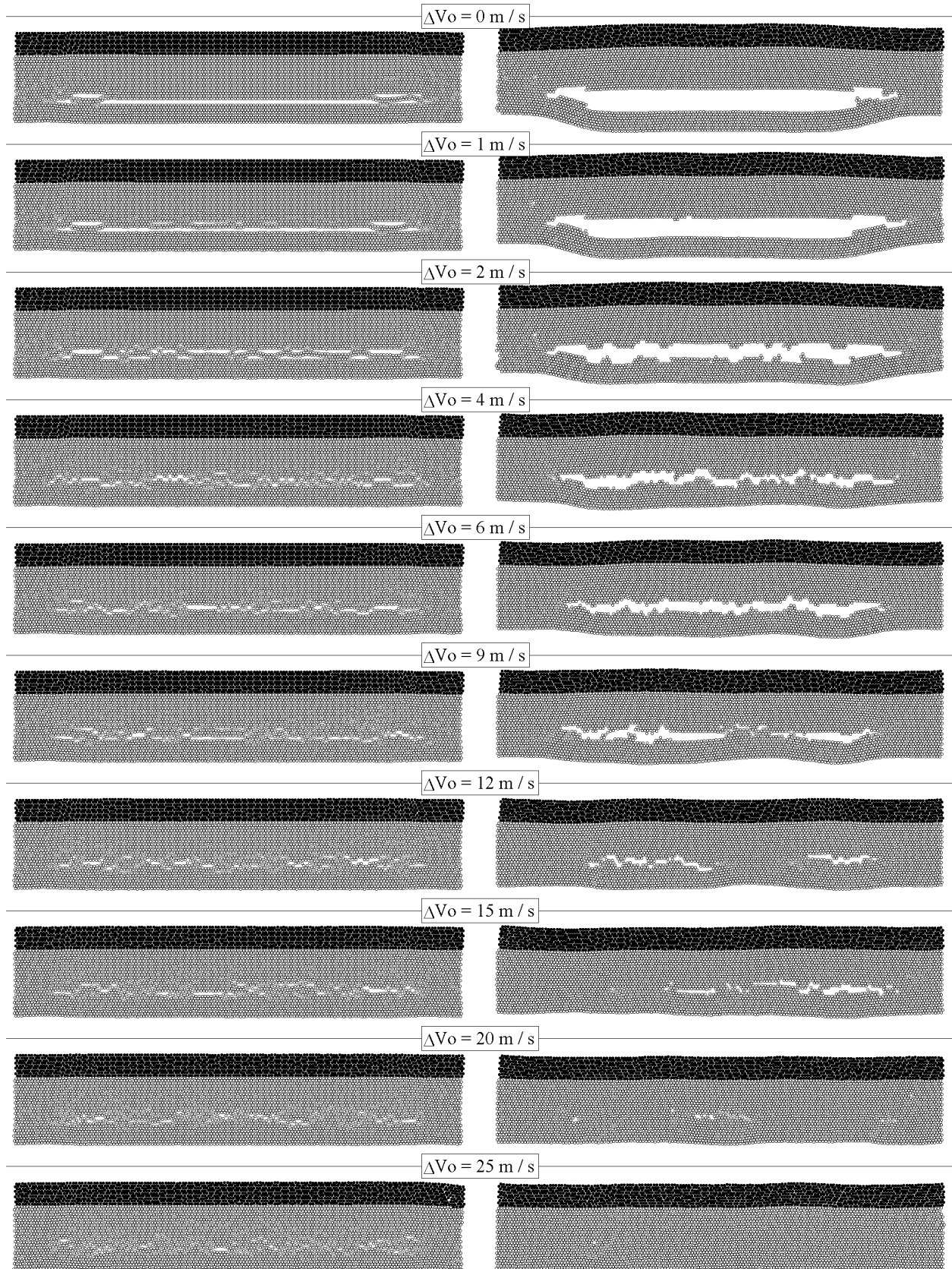


Fig. 5: Comparison of the crack state at $t = 1.4 \mu\text{s}$ (left) and $t = 4.1 \mu\text{s}$ (right column)

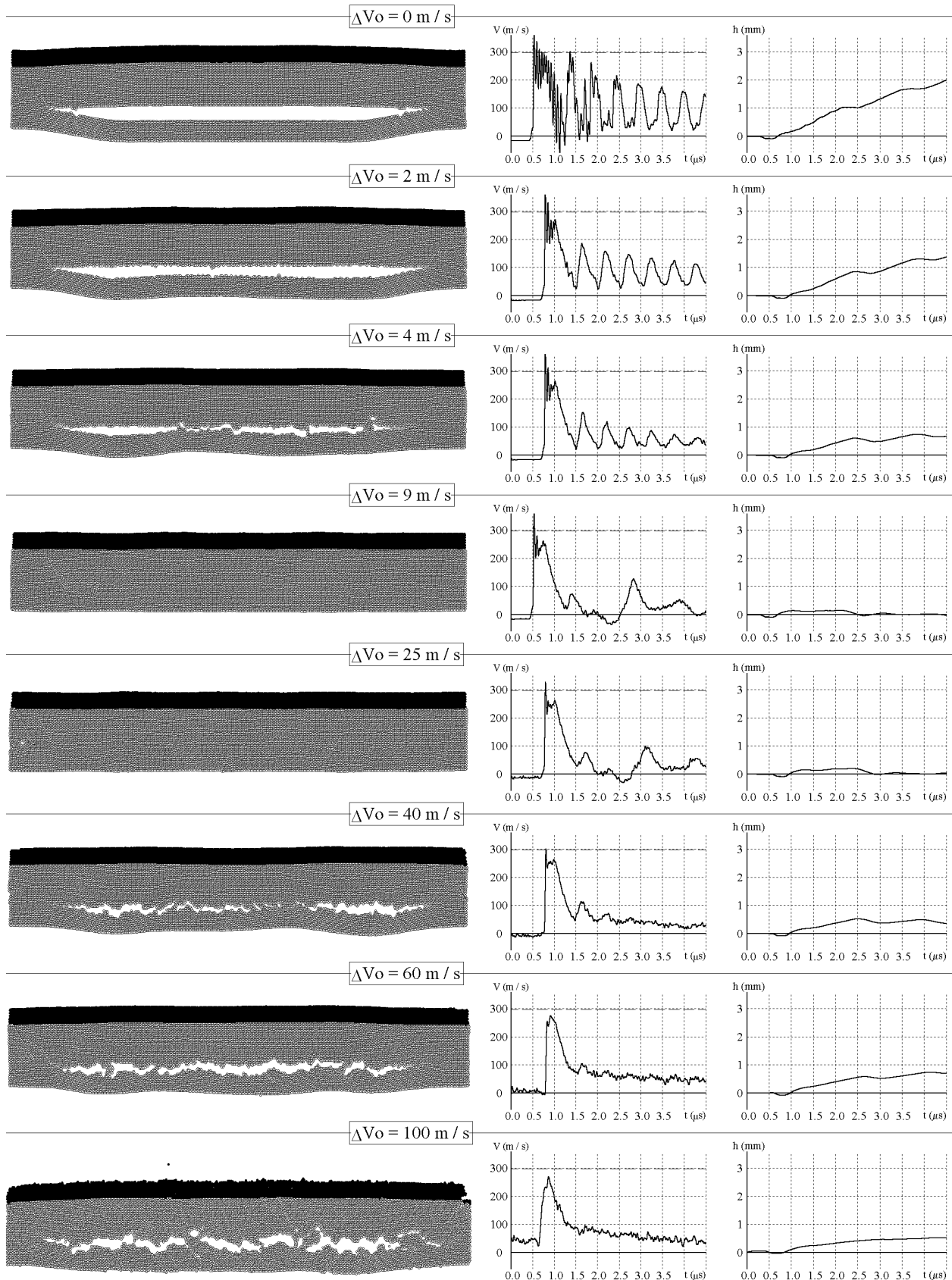


Fig. 6: Computer results for $0 \leq \Delta V_0 \leq 100 \text{ m/s}$, 20000 particles.

STRENGTH DEPENDENCE ON THE INITIAL DEVIATION

Results of all the calculations are presented in Fig. 7 where the dependence of crack width, h , and spall velocity, W , on the initial deviation is shown. Fig. 7a corresponds to experiments with 5000 particles; Fig. 7b corresponds to experiments with 20000 particles. The curve marked $h(4.1 \mu\text{s})$ shows the width of the spall crack at $4.1 \mu\text{s}$ after the first contact between impactor and target. Dots on the curves correspond to results obtained from the computer experiments. Note in Fig. 7a that the width of the spall crack sharply decreases from 2.6 mm (no initial dispersion) to zero at $\Delta V_0 = 20 \text{ m/s}$. From $\Delta V_0 = 20 \text{ m/s}$ to $\Delta V_0 = 40 \text{ m/s}$ there is no spall. After $\Delta V_0 = 40 \text{ m/s}$ the crack width increases up to 0.8 mm. For the larger system (Fig. 7b) results are the same, but the crack width decreases faster and the area without spall is shifted to the left.

The curve marked $h(1.4 \mu\text{s})$ (white dots) corresponds to the time of the microcracks appearance (the fracture's beginning). This curve actually gives the integral width of the microcracks. This dependence has the same form of the previous results, but it has far less variation: the crack width $h(1.4 \mu\text{s})$ vary from the maximum value of 0.5 mm when there is no initial dispersion to the minimum value of 0.2 mm. So, the integral width of the microcracks is more than zero for all values of dispersion, but for big dispersions microcracks disappear after some microseconds — for deviations from 12 m/s to 54 m/s the white curve lies above the black one.

The curve marked W in Fig. 7 shows the spall velocity dependence on the initial deviation. Remember that the spall (pull-back) velocity, W , is the difference between the first maximum and the first minimum on the time dependence of the free surface velocity [10]. The spall velocity is proportional to the spall strength of the material; it is one of the main strength characteristics that we can get from spall fracture experiments. From Fig. 7 note that W has a maximum at the same place where the width of the spall crack has a minimum. So the both criteria: the spall strength and the width of the spall crack give the same result. Note that to find the proper value of W , the time dependence of the free surface velocity was filtered to remove high-frequency oscillations.

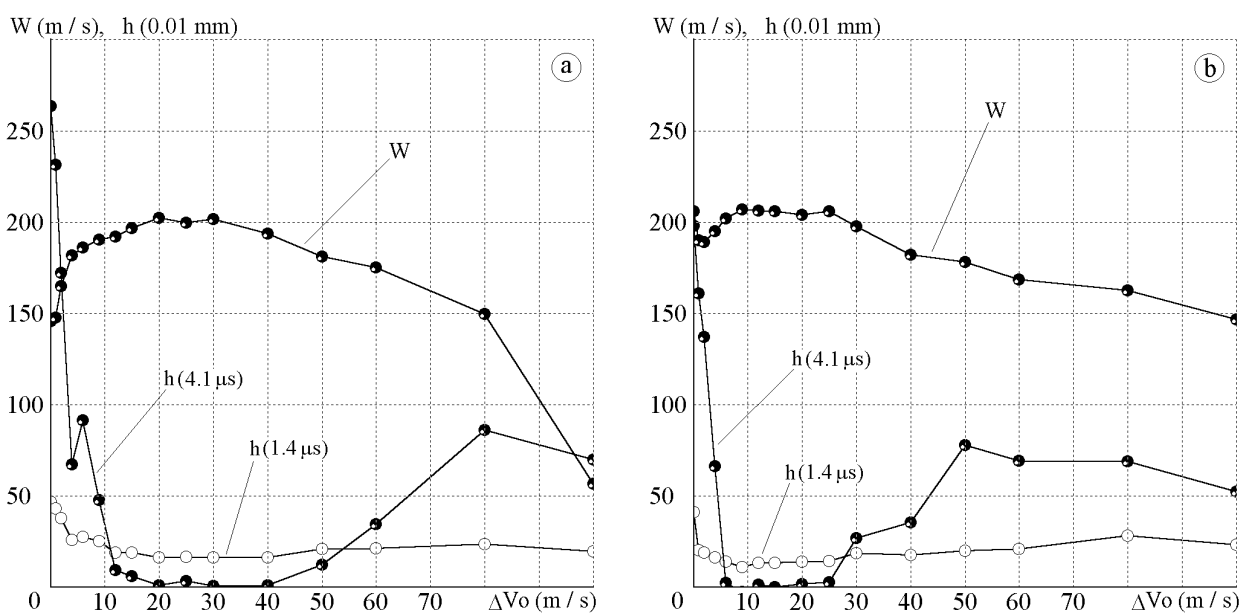


Fig. 7: The spall velocity W and the crack width h dependence on the initial deviation: experiments with a) 5000 particles, b) 20000 particles.

DISCUSSION

The presented computer simulations show that value of the initial velocity dispersion in the impact direction has a strong influence on the spall strength of material. From the analysis of the time relations of the spall crack shape it follows that there are two main reasons why the dispersion increases the material strength. The first is that dispersion reduces localisation of the shock fracture — the thickness of the fracture area is far greater when the dispersion is high. However, since the energy of the shock wave is the same, stresses in the fracture zone became far less. The second reason is that the dispersion stimulates relaxation processes in the material. The microcracks that are present at the beginning of the fracture can disappear after a few microseconds if the dispersion is high enough. These results of the computer calculations coincide with the results obtained from the real experiments with ductile steels and aluminum alloys [4, 12]. In particular in reference [4] it was shown that the mesoparticle velocity dispersion characterises the intensity of relaxation processes at the mesolevel and hence the material strength: if at the onset of spallation, the microstresses at the mesolevel have time to decrease due to relaxation processes, the material reveals the maximum possible dynamic strength.

From the computer calculations it follows that if the initial dispersion is very high, it leads to the opposite result — material strength decreases. In this case we have a situation analogous to the decrease of the material strength at high temperatures. For example, the recent spall fracture experiments with aluminum and magnesium showed precipitous drop in the spall strength of preheated samples as temperatures approached the melting point [13]. From the mesoscale point of view, high dispersion decreases the material density; the material became more porous and less stable.

The computer model used to obtain the considered results was very simple: ideal monoatomic lattice with Lennard-Jones potential. If we consider the particles as elements of microscopic scale level (for example, atoms), then the results can be interpreted in the other way: relation of dynamic strength of the monocrystal on the absolute temperature was obtained. If we consider the particles as elements of mesoscopic scale level, then instead of temperature we should use term “mesoparticle dispersion”. Of course the considered model is very crude in its description of dynamic strength properties of real solids, but the obtained results are in good agreement with the real experiment results. Hence the presented model allows describing generically the strength–dispersion relation of the real solids. For exact results more complex models are desirable, but the main tendencies should be similar.

CONCLUSIONS

1. The computer experiments show that the increase of the initial dispersion from zero to 15–25 m/s leads essentially to an increase of the material strength. The further increase of dispersion leads to the slow decreasing of the material strength, so the strength–dispersion characteristic has maximum.
2. If the initial dispersion is close to zero, the fracture is localised in a very thin layer, and borders of the spall crack are absolutely straight. The dispersion increase produced increasing of the thickness of the fracture area, and the spall crack borders became irregular. Thus the dispersion leads to smearing of the shock wave.
3. If the dispersion is great enough, the small cracks can disappear spontaneously, so dispersion stimulates the relaxation processes in the material.

4. The criterion of the spall strength, obtained from the spall (pull-back) velocity gives the same result with the criterion of the spall crack width — maximum of the spall strength corresponds to the minimum (or absence) of the spall crack width. However the criterion of the spall crack width is far more sensitive.

These conclusions are obtained from the molecular dynamics simulation, and they are in a good agreement with the results obtained from the real experiments [4, 12, 13]. In particular, the plate impact experiments [4] with ductile steels show that the maximum spall strength corresponds to the tests with the maximum mesoparticle velocity dispersion; spall fracture experiments with aluminum and magnesium show drop in the spall strength as the temperature (dispersion) approached the melting point [13]; the impact experiments and the microstructure investigation [4, 12] show that the mesoparticle velocity dispersion is strongly connected with the intensity of relaxation processes.

Acknowledgements — The author wishes to thank Professor Y. I. Mescheryakov for the experimental data and useful discussions. This work was sponsored by Army Research Laboratory, contract N DAALO1-96-M-0141. The author gratefully acknowledges HVIS98 Organizing Committee and Sandia National Laboratories for their support that made possible the author's participation in HVIS98.

REFERENCES

1. Corbett, G. G., Reid, S. R. and Johnson, W., Impact loading of plates and shells by free-flying projectiles: a review. *International Journal of Impact Engineering*, 1997, **20**, 141–230.
2. Curran, D. R. and Seaman, L., Dynamic failure of solids. *Phys. Reports*, 1987, **147**, 253–388.
3. Asay, J. R. and Barker, L. M., Interatomic measurement of shock-induced internal particle velocity and spatial variation of particle velocity. *J. Appl. Phys.*, 1974, **45**, 2545–2550.
4. Mescheryakov, Y. I. and Divakov, A. K., Multiscale kinetics of microstructure and strain-rate dependence of materials. *DYMAT J.*, 1994, **4**, 271–287.
5. Allen, M. P. and Tildesley, A. K., *Computer Simulation of Liquids*. Clarendon Press, Oxford, 1987.
6. Eckstein, W., *Computer simulation of Ion–Solid Interactions*. Springer-Verlag, Berlin Heidelberg, 1991.
7. Krivtsov, A. M., Zhilin, P. A., Particle Simulation of Large Inelastic Deformations. *Transactions of the 14th Int. Conf. on Structural Mechanics in Reactor technology (SMiRT 14)*, 1997, Lyon, France, 121–128.
8. Nagy, I., László, J., and Giber, J., *Z. Phys.*, 1985, **A321**, 221.
9. *Molecular Dynamics Simulation of Statistical-Mechanical systems*. Eds. Ciccotti, G. and Hoover, W. G., North-Holland, Amsterdam, 1986.
10. Cochran, S. and Banner, D. *J. Appl. Phys.*, 1977, **48**, 2729.
11. Chen, D., Al-Hassani, S. T. S., Sarumi, M., and Xiaogang, J., Crack straining-based spall model. *International Journal of Impact Engineering*, 1997, **19**, 107–116.
12. Mescheryakov, Y. I., Mahutov, N. A., and Atroschenko, S. A, Micromechanisms of dynamic fracture of ductile high-strength steels, *J. Mech. Phys. Sol.*, 1994, **42**, 1435–1457.
13. Kanel, G. I., Razorenov, S. V., Bogatch, A., Utkin, A. V., and Grady, D. E., Simulation of spall fracture of aluminum and magnesium over a wide range of load duration and temperature. *International Journal of Impact Engineering*, 1997, **20**, 467–478.